# A New Approach to the Assessment of Stereophonic Sound System Performance*

J. C. BENNETT, K. BARKER, AND F. O. EDEKO

*Department of Electronic and Electrical Engineering, University of Sheffield, Sheffield S1 3JD, UK*

The performance of a stereophonic sound reproduction system is considered in terms of its wavefront reconstruction capabilities. A new theory of image localization is proposed and used to develop a more general stereophonic sine law which is valid at higher frequencies. The phenomenon of central image disappearance is considered, and the resulting analysis is shown to conform with subjective experience. A criterion is established for the frequency above which a stereophonic system can no longer provide high-fidelity reproduction. Practical results are provided to substantiate the proposed theories.

## 0 INTRODUCTION

An ideal sound reproduction system is one that is capable of reconstituting the wavefronts from a particular sound scene in an exact form over a region of space occupied by a listener. The recording and replay processes involved must be holosonic in nature so that they are capable of adequately sampling and regenerating the wide temporal and spatial bandwidths encountered in practice. The two-loudspeaker stereophonic system approximates these requirements and provides what is generally considered as an acceptable and economical form of reproduction system. However, the use of only two spatially separated loudspeakers necessarily imposes restrictions on the ability of stereophony to reconstruct the correct acoustic wavefronts. As will be seen later, a typical system can provide only one centrally located listener with correctly reproduced sound information up to a frequency of around 1100 Hz. It is therefore hardly surprising that even a sophisticated two-loudspeaker modern system still cannot offer the true experience of the original sound scene. During recent decades much thought has been given to the spatial aspects of sound reproduction [1]–[12], and considerable progress has been made in optimizing the performance of recording and replay equipment over the complete audio range. However, comparatively few efforts have been made to address the problem of the wavefront reconstruction process which is so vital to the human experience. This contribution is intended to provide a new approach to the assessment of stereophonic sound system performance and suggests principles that could be employed in the consideration of more general multichannel configurations.

## 1 STEREOPHONIC REPRODUCTION AS A WAVEFRONT RECONSTRUCTION PROCESS

The ear–brain combination bases its assessment of a sound scene on the information available from a spatially limited sample of the complex wavefront propagating toward the head. One of the primary functions of a sound reproduction system is to re-create such wavefronts so that they provide directional cues to the listener and enable the listener to specify the angular location of the source. The nature of the wavefront corresponding to a real (or virtual) source is therefore of interest. Fig. 1 shows the geometry involved for a source located in a direction $\alpha$ at distance $R_0$ from a listener. Here, for $x << R_0$,

$$r \simeq R_0 + \frac{x^2}{2R_0} + x \sin \alpha \qquad (1)$$

and as $R_0 \rightarrow \infty$, $r = R_0 + x \sin \alpha$. The wavefront $f(x)$ along the $x$ axis becomes a plane wave and can be described as

$$f(x) = \tilde{A} \exp [jkx \sin \alpha] \qquad (2)$$

where $\tilde{A}$ is a complex constant incorporating the effective amplitude and absolute phase of the wavefront,

* Manuscript received 1984 July 9; revised 1985 January 14.

$k = 2\pi/\lambda$ is the propagation constant, and $\lambda$ is the wavelength measured along the direction of propagation.

In assessing the performance of a reproduction system it is constructive to decompose the complex wavefront $H(x)$ at the head into a set of plane wave components so that

$$H(x) \simeq \sum_{i=1}^{N} \tilde{A}_i \exp [jkx \sin \alpha_i] \ . \quad (3)$$

Each component can then be interpreted as a source of amplitude and phase $\tilde{A}_i$ located at $\alpha_i$ and so provide details of the composite source distribution apparent to the listener at the frequency of interest. Such a technique provides a more rigorous interpretation of the situation than earlier approaches, which only take account of the phase difference at the ears [1], [4], [6], [10], [12].

## 2 IMAGE LOCALIZATION

For a two-channel stereophonic system it is usually required that only one virtual source be created for each real source present in the original sound scene. If the prime function of the ear and brain is to assign a specific location to such a source, then a procedure is required to extract the predominant plane wave component from $H(x)$. Consider now the wavefront $H(x)$ produced by a stereophonic system. From the geometry of Fig. 2, for left and right loudspeaker amplitudes $L$ and $R$, respectively, the acoustic distribution along $x$ is given by

$$H^1(x) = L \exp [jkr_1] + R \exp [jkr_2] \quad (4)$$

where radial amplitude reductions in the divergent wavefronts and loudspeaker polar diagram variations are assumed small over the region occupied by the head. From Eq. (1),

$$H^1(x) = \exp \left[ jk\left(R_0 + \frac{x^2}{2R_0}\right)\right]\{L \exp [jkx \sin \vartheta_0] + R \exp [- jkx \sin \vartheta_0]\} \ . \quad (5)$$

The common multiplicative phase term can be ignored because it carries no significant directional information, and so

$$\begin{aligned} H(x) &= L \exp [jkx \sin \vartheta_0] + R \exp \\ &\quad \times [- jkx \sin \vartheta_0] \\ &= 2L \cos (kx \sin \vartheta_0) \\ &\quad + [R - L] \exp [- jkx \sin \vartheta_0] \ . \end{aligned} \quad (6)$$

The phase $\varphi(x)$ of $H(x)$ is of interest because it is this which determines the apparent direction of the virtual image:

$$\begin{aligned} \varphi(x) &= \arctan [(L - R)\sin (kx \sin \vartheta_0)] \\ &\quad \times [2L \cos (kx \sin \vartheta_0) \\ &\quad + (R - L) \cos (kx \sin \vartheta_0)]^{-1} \ . \end{aligned} \quad (7)$$

For low frequencies $x_m << \lambda$, where $2x_m$ is the width of the head, and therefore Eq. (7) can be simplified to

$$\varphi(x) = \frac{L - R}{L + R} kx \sin \vartheta_0 \ . \quad (8)$$

Now if $\alpha$ is the apparent direction of the virtual image, then from Eq. (2) the expected rate of change of phase with $x$, $d\varphi_v/dx$, is

$$\frac{d\varphi_v}{dx} = k \sin \alpha \quad (9)$$

and from Eq. (8) the rate of change of phase produced by the stereo pair is

$$\frac{d\varphi}{dx} = \frac{L - R}{L + R} k \sin \vartheta_0 \ . \quad (10)$$

Equating Eqs. (9) and (10),

$$\sin \alpha = \frac{L - R}{L + R} \sin \vartheta_0 \quad (11)$$

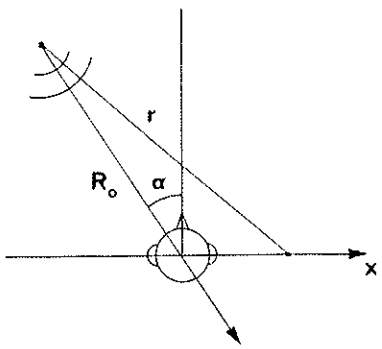


Fig. 1. Listener in presence of real source.

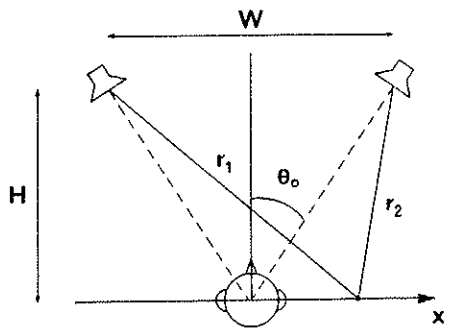


Fig. 2. Stereophonic system geometry.

which is the well-known stereophonic law of sines [5], [13].

Eq. (11) provides a useful means for predicting the virtual image direction, although other schemes can be used to determine the dominant plane wave component. For example, the linear variation of the phase component of $f(x)$ suggests the use of a least-squares approach to obtain the best-fit phase slope for a particular wavefront.

A further technique, which leads toward a more precise localization formula, can be developed by using the geometry of Fig. 3. Here the acoustic field distribution is considered over a circular path of radius $a$, which is just large enough to encompass the head. This distribution, $H(\vartheta)$, due to the two loudspeakers located at $\vartheta = \pm\vartheta_0$, is compared with a second wavefront $I(\vartheta)$, which would be produced by a distant virtual source located at angle $\alpha$. The ability of $I(\vartheta)$ to match $H(\vartheta)$ is achieved by varying $\alpha$ to minimize the difference between the two wavefronts over the region $-\pi/2 \leqq \alpha \leqq \pi/2$, that is, over the forward hemisphere of the head in the direction of the virtual source.

In this analysis the low-frequency case is considered, and once again $1/r$ space attenuation changes and loudspeaker polar diagram variations are assumed small over the region occupied by the head. Excluding constant phase terms, the left loudspeaker creates a wavefront over the circular path which is given by

$$\begin{aligned} L(\vartheta) &= L \exp\,[j(2\pi a/\lambda)\cos(\vartheta - \vartheta_0)] \\ &\simeq L[1 + jT(\cos\vartheta\cos\vartheta_0 \\ &\quad + \sin\vartheta\sin\vartheta_0)] \end{aligned} \tag{12}$$

where $T = 2\pi a/\lambda$ and it has been assumed that $a << \lambda$. Similarly for the right loudspeaker,

$$R(\vartheta) = R[1 + jT(\cos\vartheta\cos\vartheta_0 - \sin\vartheta\sin\vartheta_0)] \tag{13}$$

and the combined wavefront $H(\vartheta)$ is

$$\begin{aligned} H(\vartheta) &= L(\vartheta) + R(\vartheta) \\ &= L + R + jT[(L + R)\cos\vartheta\cos\vartheta_0 \\ &\quad - (R - L)\sin\vartheta\sin\vartheta_0)] \,. \end{aligned} \tag{14}$$

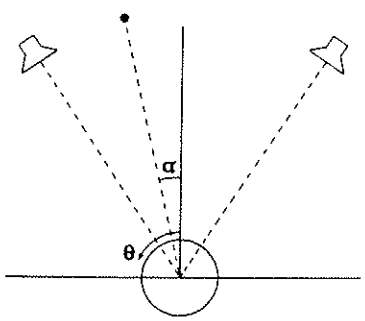


Fig. 3. Geometry for wavefront difference minimization.

The virtual source wavefront $I(\vartheta)$ is

$$I(\vartheta) = A[1 + jT(\cos\vartheta\cos\alpha + \sin\vartheta\sin\alpha)] \,. \tag{15}$$

Since, for the above condition of $a << \lambda$, the imaginary part of $H(\vartheta)$ is small compared with $L + R$, then it is reasonable to set $A = L + R$ so that $I(\vartheta)$ and $H(\vartheta)$ have substantially the same magnitude.

The difference between the two wavefronts as $\alpha$ is varied can now be expressed as

$$\begin{aligned} D(\alpha) &= \int_{\alpha-\pi/2}^{\alpha+\pi/2} |H(\vartheta) - I(\vartheta)|\,d\vartheta \\ &= T\int_{\alpha-\pi/2}^{\alpha+\pi/2} [(L + R)\cos\vartheta\cos\vartheta_0 \\ &\quad - (R - L)\sin\vartheta\sin\vartheta_0 \\ &\quad - (L + R)(\cos\vartheta\cos\alpha \\ &\quad + \sin\vartheta\sin\alpha)]\,d\vartheta \\ &= 2T[(L + R)\cos\alpha\cos\vartheta_0 \\ &\quad + (L - R)\sin\alpha\sin\vartheta_0 \\ &\quad - (L + R)] \,. \end{aligned} \tag{16}$$

Minimum difference occurs when the first derivative of $D(\alpha)$ with respect to $\alpha$ is set to zero, and this leads to the condition

$$\tan\alpha = \frac{L - R}{L + R}\tan\vartheta_0 \,. \tag{17}$$

Interestingly, this formula is identical to one previously developed by assuming that the brain is sensitive to interaural time difference and its variation with head movement [14].

Eq. (17) is valid for frequencies up to about 500 Hz, beyond which higher order terms in the approximation to Eq. (12) must be taken into account.

The above technique has also been implemented in software and no assumptions were made in the generation of $H(\vartheta)$. In this case the rms difference between $H(\vartheta)$ and $I(\vartheta)$ was minimized for $-\pi/2 \leqq \alpha \leqq \pi/2$, and the results showed very good agreement with Eq. (1) for frequencies up to 500 Hz.

Such schemes are of interest because they enable frequency and head size to be incorporated as variable parameters. Furthermore, the minimization methods enable the amplitude to be included in the process, thus allowing a more comprehensive approach.

These procedures have been investigated computationally for the geometry of Fig. 2. In each case the polar response of the loudspeaker was assumed to be omnidirectional since this introduces negligible effects when the free-field situation is being considered. Polar patterns can be incorporated if necessary. The software

involved generates the amplitude and phase of $H(x)$ or $H(\varphi)$ for specified left and right channel amplitudes, frequency, system geometry, and head size. Comparisons have been made between the computer-predicted results, Eq. (17), those obtained from listening tests carried out by Leakey [6], [14], and from the authors' practical results.

Fig. 4 shows the corresponding variations of virtual image position with interchannel intensity difference for the low-frequency case (250–500 Hz). Tests were carried out in an anechoic chamber with a reverberation time of less than 0.25 s for frequencies down to 125 Hz. The signal used for all subjective tests was one-third-octave pink noise produced by a random noise signal generator in conjunction with a bandpass filter set (Bruel & Kjaer types 1402 and 1611). Each loudspeaker cabinet housed a single type 8P unit produced by Goodmans Loudspeakers Ltd., and 12 listeners participated in the investigations. It can be seen that in each case the stereophonic law of sines and the phase-only results are similar, but each underestimates the virtual image displacement for a given intensity difference. However, when the minimization approaches are used, the procedure allows a more complete characterization, and a very good correspondence exists between predicted and experimental results.

## 3 CENTRAL IMAGE DISAPPEARANCE

It is useful to consider further the possibility of decomposing the sound field into its separate spatial components for the case of equally driven loudspeakers. From Eq. (6), when $L = R = 1$,

$$H(x) = 2 \cos (kx \sin \vartheta_0) \tag{18}$$

for $-x_m \leqq x \leqq x_m$. For the case of $x_m << \lambda$ (low frequencies), $H(x)$ is approximately constant and the head is immersed in a high-quality plane wave apparently emanating from a distant source at $\alpha = 0$. As the frequency is increased, $H(x)$ acquires an amplitude taper and the effective source distribution required to

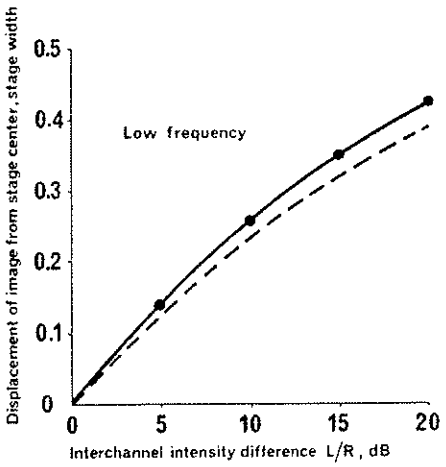


Fig. 4. Variation of virtual image position at low frequencies. — Leakey [14] and this work, $W = 2.3$ m, $\theta_0 = 30°$; -- Law of sines and best-fit phase; •• minimization.

constitute $H(x)$ becomes more diverse. In order to deduce the spatial frequencies composing $H(x)$ it is now defined that $H(x)$ forms one period of a repetitive function $H(x) * \mathrm{III}(x/2x_m)$, where * denotes convolution and $\mathrm{III}(x/2x_m)$ is a comb function with period $2x_m$ [15]. Under such circumstances the head will still sense $H(x)$ alone because of the band-limited nature of the process, that is, the head will act as a finite collecting aperture defined by rect $(x/2x_m)$, and the wavefront experienced will be

$$H_e(x) = [H(x) * \mathrm{III}(x/2x_m)] \text{ rect } (x/2x_m) = H(x) . \tag{19}$$

The following series expansion can be exploited for noninteger values of $Q$:

$$\cos \frac{Qx\pi}{x_m} = \frac{2Q}{\pi} \sin Q\pi \left\{ \frac{1}{2Q^2} + \sum_{n=1}^{\infty} (-1)^{n-1} \frac{\cos (nx\pi/x_m)}{n^2 - Q^2} \right\} \tag{20}$$

where $Q = (2x_m \sin \vartheta_0)/\lambda$ and $-x_m \leqq x \leqq x_m$. (Integer values of $Q$ lead to simple solutions.)

A typical harmonic component of Eq. (20) has the spatial variation

$$g(x) = 2B \cos (nx\pi/x_m) = B \exp[jnx\pi/x_m] + B \exp [-jnx\pi/x_m] \tag{21}$$

which can be interpreted as a pair of plane wave components with phase slopes of $\pm n\pi/x_m$. Using Eq. (9), the directions of the corresponding virtual sources are found to be

$$\sin \alpha = \pm \frac{n\lambda}{2x_m} . \tag{22}$$

Both the virtual source amplitude and its direction are frequency dependent, and Fig. 5 shows the migration of the sources which occurs in the region $\alpha = \pm 90°$ for a head diameter of 140 mm and $\vartheta_0 = 30°$. Several interesting effects are seen here. As the frequency increases, there is a reduction in the central image and side sources appear at $\pm 90°$. These side sources correspond to the case of listening to side-located loudspeakers or through headphones and would be expected to generate in-the-head images because there is no forward ($\alpha < 90°$) component of the wavefront incident on the ear. At a particular frequency, as shown in Fig. 5(g), a complete period of the interference pattern exists across the head. Under this condition the central image disappears, and a source appears located at each loudspeaker. A further increase in the frequency causes further source movement, and finally all components cluster around the location of the loudspeakers.

In order to confirm these predictions, tests have been carried out using subjects with differing head widths located at different values of $\vartheta_0$ relative to a pair of identical in-phase equal-amplitude loudspeakers. Listeners were asked to identify the frequency at which disappearance of the central image occurred, and the results obtained for a set of listeners with almost the same head width of 140 mm are shown in Fig. 6. A very good correspondence is seen between theory and experiment, and it is also significant that in arriving at their decisions, subjects were confused by the appearance of in- and over-the-head virtual images. Once again, one-third-octave pink noise was used for the tests, and it is interesting to note that listeners sometimes considered that the side images possessed higher frequency components than the central image—as the theory would suggest.

## 4 DETERMINATION OF UPPER FREQUENCY LIMIT

The ability of a stereophonic system to produce an on-axis ($\alpha = 0$) plane wave gives some indication of the upper frequency limit at which its performance becomes unacceptable. The case of $\alpha = 0$ is chosen because this is found to be the most severe test for the system; as virtual images are moved away from the stage center, it becomes increasingly easy to re-create the required wavefront until in the limit the virtual source becomes a real source when only one loudspeaker is radiating.

A measure of the acceptability of the plane wave is the rms level of the residual information in the wavefront, which cannot be assigned to the on-axis component, and this corresponds to unwanted sources at other directions in space. Fig. 7 shows typical results obtained by computation of the residual information present in $H^1(x)$ from Eq. (4), with spreading loss included, and clearly indicates the degradation of the on-axis component with increasing frequency. Here the wavefront is assessed only over the 140-mm region occupied by the head of a centrally located listener; inferior results would be expected at other positions in space. It is clear from the figure that improved frequency response can be obtained at the expense of stage width, which is to be expected from consideration of the spatial sampling criterion.

The unacceptable rms level can be considered as the one that corresponds to the appearance of additional sound sources which modify the sound scene beyond

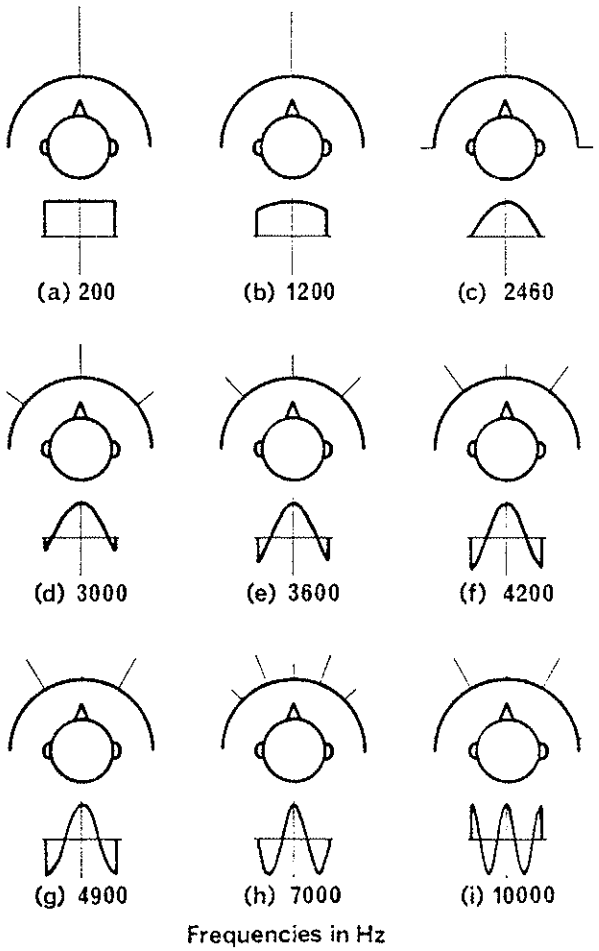


Fig. 5. Migration of apparent source distribution. Radial lines represent position and magnitude of apparent sources; $H(x)$ shown for each case.

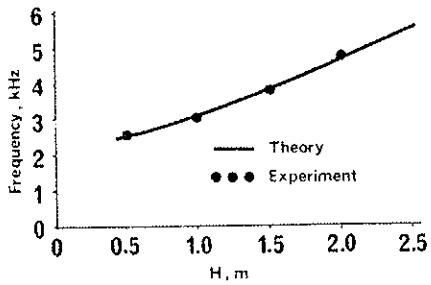


Fig. 6. Disappearance of central image. $W = 2.3$ m.

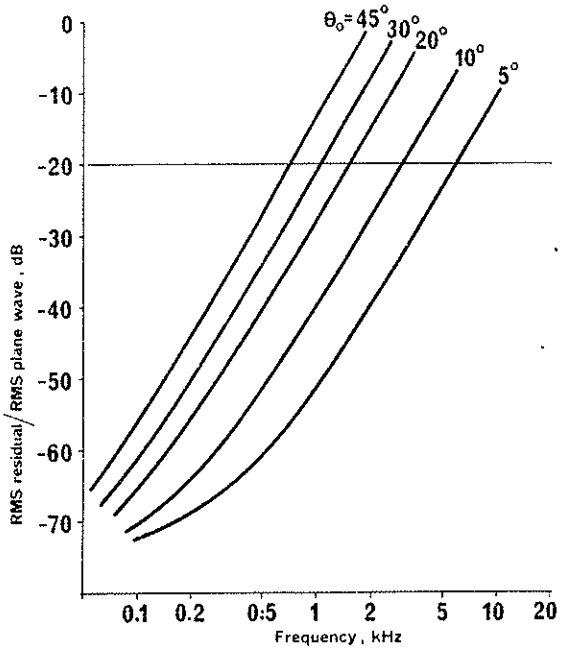


Fig. 7. Residual content of plane wave.

that of a single central image. Practical investigations have been carried out to determine the upper frequency limit of a stereophonic sound reproductive system on the basis of the above criterion. For the geometry of Fig. 2 a third identical loudspeaker was introduced at stage center to provide a real source for comparison with the phantom image produced by the stereo pair of loudspeakers. The loudness levels of the phantom and real sources were equalized and compared for several values of $\vartheta_0$. It was found that the upper frequencies at which degradation of the phantom image first became perceptible were about 850 Hz ($\vartheta_0 = 45°$), 1100 Hz ($\vartheta_0 = 30°$), and 1700 Hz ($\vartheta_0 = 20°$). Using these results with Eq. (20) or Fig. 7, the corresponding rms value of the unwanted residual information can be obtained and used to specify a −20-dB level for minimum acceptable quality. Previous work [16] refers to a figure of $L/R = -19$ dB as that required to shift the image just away from one loudspeaker. It is worth noting that this level, which corresponds to a minimum perceptible change in the effective source distribution, agrees well with the value specified above.

## 5 A MORE GENERAL APPROACH TO THE STEREOPHONIC SINE LAW

In deriving the low-frequency stereophonic law of sines, Eq. (11), certain assumptions were made which become invalid at higher frequencies. However, the Fourier analysis given earlier can be further exploited to develop a higher frequency version of Eq. (11) by expanding the cosine term of Eq. (6). From the theory relating to Fig. 5 it is found that for frequencies up to around 3 kHz the term can be decomposed into a constant and a first harmonic. These correspond to a central on-axis image and two other single, equal-amplitude sources at wide angles. Considering these latter as headphone or side-loudspeaker sources, it can be assumed that they will only give rise to a central in-the-head effect and not contribute to forward directional information. The factor remaining is a constant term similar to that of the low-frequency case, but of reduced amplitude. This, combined with the linear phase term of Eq. (6), will give the required directional information. Because of the reduced "central source" amplitude, it will be anticipated that at high frequencies a greater image shift will occur for a given $L/R$ ratio. The phase $\varphi(x)$ now becomes

$$\varphi(x) = \arctan\left[(L - R)\sin(kx\sin\vartheta_0)\right] \times \left[2L(\sin Q\pi/Q\pi) + (R - L)\cos(kx\sin\vartheta_0)\right]^{-1} . \quad (23)$$

Eq. (23) holds for $R \geqq L$. To deal with cases where $L \geqq R$, the terms $R$ and $L$ must be interchanged. Making the assumption that the same approximations can be made here as at low frequencies,

$$\sin\alpha = \frac{L - R}{2L(\sin Q\pi/Q\pi) + R - L}\sin\vartheta_0 . \quad (24)$$

Eq. (24) is a more general version of the stereophonic sine law and is seen to reduce to Eq. (11) as the frequency tends to zero. However, as the frequency increases, the approximations used cause Eq. (24) to become less accurate. Therefore in order to extend the usable range of this new analysis, the best-fit slope is deduced from Eq. (23) by least squares and used to deduce the virtual source distribution.

Comparisons have been made between the computer-predicted results and those obtained from listening tests. The frequency chosen was 2500 Hz, and the comparisons are shown in Fig. 8 together with Leakey's high-frequency results. Good agreement exists between theory and experiment in each case. Computer predictions for two typical head widths and the band limits of frequency presented to the listeners are provided to demonstrate the significance of these parameters.

The more general approach implicit in Eq. (23) can be used to investigate the relationship between low- and high-frequency values of sin $\alpha$, which has been reported previously in practical tests [5]. As Eqs. (23) and (24) show, the relative image shift obtained is dependent on interchannel intensity difference as well as frequency. Taking the case of $L = 3R$, the predictions of image position versus frequency are shown in Fig. 9. As might be expected, it is clear that the effect is gradual rather than possessing a specific high-to-low-frequency ratio.

## 6 CONCLUSIONS

In conclusion it has been shown that a more complete appreciation of sound system performance can be obtained by considering the characteristics of the acoustic wavefront incident on a listener. The size of the head plays an important role in the determination of the apparent sound scene, and the brain bases its assessment on the information contained in a section of wavefront which is some 140 mm in extent. It is this spatially band-limited interpretation that permits the use of a

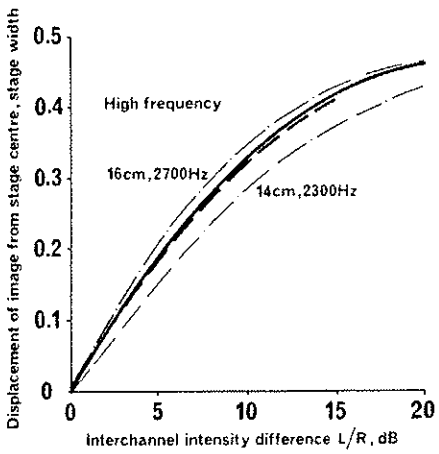


Fig. 8. Variation of virtual image position at high frequencies. — this work; ---Leakey [14]; ·-· law of sines with best-fit lines.

two-loudspeaker (stereophonic) reproduction system. At low frequencies such a system is capable of generating a substantially plane wave in the region of the listener, with a tilt or phase slope determined by the interchannel intensity difference. Such a wavefront is characteristic of a single, distant source emanating from an angular location within the sound stage bounded by the loudspeakers. This feature allows the linearity of the system to be exploited so that many spatially distributed sources can be reconstructed from two channels of information. In this contribution the wavefront approach has been used to redevelop the stereophonic law of sines and to introduce numerical techniques which have permitted a more accurate prediction of the low-frequency listening experience.

At higher frequencies the stereophonic system can no longer maintain its low-frequency performance, and it has been shown that for the case of equal loudspeaker amplitudes, reduction of the central image amplitude occurs. A theory has been developed to explain this degradation in terms of a migratory effective source distribution, and practical results are presented to substantiate the predictions.[1]

A more general version of the stereophonic law of sines has been developed and used successfully to predict high-frequency image positions and quantify the relationship known to exist between low- and high-frequency image displacements.

Future work will be directed toward further refinement of the above techniques. Additional areas to be examined include the effects of phase shift between channels, a theory for image broadening, the influence of room acoustics, and explanations for effects experienced by an off-center listener. Results from the wavefront reconstruction approach will be compared with previously reported work [12], [16]–[18]. Attention will also be paid to methods of improving the performance of present systems in light of these investigations in order to complement other contributions and developments already made in this area [8], [9], [19]–[21].

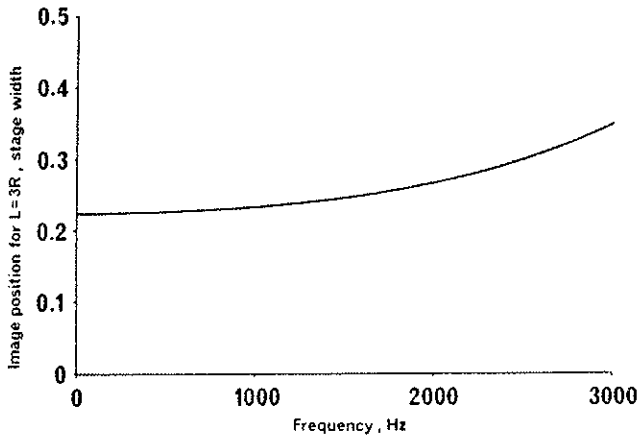


Fig. 9. Frequency dependence of image position.

[1] Throughout this work the velocity of sound has been assumed to be 343 m/s, but it is recognized that in practice variations can occur and could account for some of the discrepancies observed.

## 7 REFERENCES

[1] K. de Boer, "Stereophonic Sound Reproduction," *Philips Tech. Rev.*, vol. 5, no. 4, pp. 107–114 (1940).

[2] J. Moir and J. A. Leslie, "The Stereophonic Reproduction of Speech and Music," *J. Brit. IRE*, pp. 360–366 (1952 June).

[3] W. B. Snow, "Basic Principles of Stereophonic Sound," *J. SMPTE*, vol. 61, pp. 567–589 (1953).

[4] T. T. Sandel, D. C. Teas, W. E. Feddersen, and L. A. Jeffress, "Localization of Sound from Single and Paired Sources," *J. Acoust. Soc. Am.*, vol. 27, pp. 842–852 (1955 Sept.).

[5] H. A. M. Clark, G. F. Dutton, and P. B. Vanderlyn, "The Stereosonic Recording and Reproducing System," *IEE Proc.*, vol. 104, pt. B, pp. 417–432 (1957 Sept.).

[6] D. M. Leakey, "Stereophonic Sound Systems," *Wireless World*, vol. 66, pp. 154–160 (1960 Apr.).

[7] Y. Makita, "On the Directional Localisation of Sound in the Stereophonic Sound Field," *EBU Rev.*, pt. A, pp. 102–108 (1962 June).

[8] M. A. Gerzon, "Surround Sound Psychoacoustics," *Wireless World*, vol. 80, pp. 483–486 (1974).

[9] M. A. Gerzon, "NRDC Surround-Sound System," *Wireless World*, vol. 83, pp. 36–39 (1977).

[10] J. M. Kates, "Optimum Loudspeaker Directional Patterns," *J. Audio Eng. Soc.*, vol. 28, pp. 787–794 (1980 Nov.).

[11] J. L. Bauck and D. H. Cooper, "On Acoustical Specification of Natural Stereo Imaging," presented at the 66th Convention of the Audio Engineering Society, *J. Audio Eng. Soc. (Abstracts)*, vol. 28, p. 552 (1980 July/Aug.), preprint 1649.

[12] J. Blauert, *Spatial Hearing*, J. S. Allen, transl. (MIT Press, Cambridge, MA, 1983).

[13] B. B. Bauer, "Phasor Analysis of Some Stereophonic Phenomena," *J. Acoust. Soc. Am.*, vol. 33, pp. 1536–1539 (1961 Nov.).

[14] D. M. Leakey, "Some Measurements on the Effects of Interchannel Intensity and Time Differences in Two Channel Sound Systems," *J. Acoust. Soc. Am.*, vol. 31, pp. 977–986 (1959 July).

[15] R. N. Bracewell, *The Fourier Transform and Its Applications* (McGraw-Hill, New York, 1978).

[16] H. D. Harwood, "Stereophonic Image Sharpness," *Wireless World*, vol. 74, pp. 207–211 (1968).

[17] T. K. Matsudaira and T. Fukami, "Phase Difference and Sound Image Localization," *J. Audio Eng. Soc.*, vol. 21, pp. 792–797 (1973 Dec.).

[18] G. F. Dutton, "The Assessment of Two-Channel Stereophonic Reproduction Performance in Studio Monitor Rooms, Living Rooms and Small Theatres," *J. Audio Eng. Soc.*, vol. 10, pp. 98–105 (1962).

[19] N. Sakamoto, T. Gotoh, T. Kogure, M. Shimbo, and A. H. Clegg, "Controlling Sound-Image Localization in Stereophonic Reproduction," *J. Audio Eng. Soc.*, vol. 29, pp. 794–799 (1981 Nov.).

[20] N. Sakamoto, T. Gotoh, T. Kogure, M. Shimbo, and A. H. Clegg, "Controlling Sound-Image Localization in Stereophonic Reproduction: Part II," *J. Audio Eng. Soc.*, vol. 30, pp. 719–722 (1982 Oct.).

[21] Y. Hirata, "Improving Stereo at l.f.," *Wireless World*, vol. 89, pp. 60–62 (1983).

## THE AUTHORS

J. C. Bennett

John C. Bennett was born in Bolsover, UK, in 1944. He received B.Eng. and Ph.D. degrees from the University of Sheffield, UK, in 1970 and 1974, respectively. Since 1972 he has been a lecturer and senior lecturer in the department of electronic and electrical engineering of the University of Sheffield. His research interests involve the wavefront analysis of multichannel sound reproduction systems, three-dimensional ultrasonic and microwave imaging, microwave holographic metrology of reflector antennas, and near-field/far-field transformation techniques. He is a member of the Institution of Electrical Engineers.

•

Keith Barker earned B.Eng. (1963) and Ph.D. (1966) degrees from the University of Sheffield, UK, where he worked on impedance and noise characteristics of gaseous discharges. Since that time he has taught electrical engineering and computer science subjects in England, Malta, and at the University of Connecticut in the USA, often with major audio and television instructional components. He has a strong professional interest in the presentation of technical information which together with his lifetime interest in high-fidelity sound recording and reproduction led him into a number of courses and a 13-year series of extramural lectures on multichannel sound. These were supported technically by many British, European, American, and Japanese manufacturers. He has continuing contact with work on psychoacoustics and the locatability of sound images, though at present he is concerned with educational innovation in digital design laboratories. He has presented papers on multichannel sound at many institutional meetings and has written for *HiFi News*, *The Gramophone* and other journals. He is a member of the Institution of Electrical Engineers, The Institute of Electrical and Electronics Engineers, and the American Society for Engineering Education.

Dr. Barker's photograph was not available at press time.

F. O. Edeko

•

Frederick O. Edeko was born in Benin-City, Nigeria, in 1952. He received an M.Sc. degree in electronics from Leningrad's Institute of Motion Picture Engineers in 1979, specializing in the design, installation and maintenance of electroacoustic and television equipment. He joined the University of Benin, Nigeria, as a lecturer in 1980 and is at present engaged in Ph.D. research work in stereophonic sound reproduction at Sheffield University, UK.